E911 钢焊接接头 650 ℃长期时效后组织与性能

任文超[1]， 龚正春[2]， 常铁军[3]， 王春斌[3]
(1. 哈尔滨工程大学 机电工程学院，哈尔滨 150001；
2. 哈电集团(秦皇岛)重型装备有限公司，河北 秦皇岛 066206；
3. 哈尔滨工程大学 材料科学与化学工程学院，哈尔滨 150001)

任文超

摘 要：对德国 Vallourec &Mannesmann 公司生产的 E911 钢焊接接头在650 ℃长期时效后进行了力学性能、系列冲击试验，并对 E911 钢焊接接头在650 ℃高温持久强度进行了测试。采用光学显微镜、透射电镜、扫描电镜对焊缝的显微组织及断口进行了观察和分析。结果表明，E911 钢焊接接头在650 ℃长期时效后仍表现出好的力学性能和持久强度，E911 钢母材在650 ℃高温外推10^5 h的持久强度 R_{10^5}＝72.52 MPa，E911 钢焊接接头在650 ℃外推10^5 h的高温持久强度为 R_{10^5}＝60.88 MPa。

关键词：E911 钢；长期时效；持久强度；显微组织；力学性能
中图分类号：TG142.73 文献标识码：A 文章编号：0253－360X(2008)08－0105－04

0 序 言

随着锅炉蒸汽温度及压力的增加，要求有更高持久强度的新钢种以提高锅炉的效率，减少能源的浪费。从目前世界各国高蒸汽参数发电机组的发展来看，电站锅炉耐热钢的研究方向是发展蠕变强度高于 T91/P91 的非热交换厚壁件以替代奥氏体不锈钢。E911 是在 T91(P91)之后由欧洲多个国家研究设计的新钢种，E911 钢的使用温度可达600 ℃，并可使壁厚减薄，使焊接容易进行，是目前超超临界锅炉钢的最有希望的钢种，同时还具有较大的经济效益[1]。此外，E911 的高温蠕变断裂强度超过 TP300 系的奥氏体不锈钢，具有优良的断裂韧性、抗热腐蚀性、可加工性、可焊性，引起了人们的极大关注[2]。

随着国内电站锅炉向大容量、高参数方向迅猛发展，锅炉行业在制造大容量、高参数亚临界和超超临界锅炉所需要的 E911 钢必将越来越多，为此，锅炉行业迫切希望钢管生产企业能研制和大批量生产 E911 钢以替代进口产品，因此，掌握 E911 钢的焊接工艺及焊后的力学性能就显得尤为重要。

1 试验方法

1.1 试验材料

试验所使用的 ϕ159 mm× 27 mm E911 钢管材料是由 Vallourec &Mannesmann 公司为哈尔滨锅炉厂提供的，炉号为 79506，供货状态为1 070 ℃/0.5 h空冷＋770 ℃/1 h空冷，其化学成分见表 1。

表 1 E911 钢的化学成分(质量分数，%)
Table 1 Chemical composition of E911 steel

C	Si	Mn	P	S	Cr	Mo
0.12	0.20	0.47	0.015	0.002	8.62	0.94
W	Ni	V	Nb	N	Al	B	Fe
0.959	0.24	0.203	0.084	0.075	0.016	0.001 8	余量

1.2 试验方法

试验的所有力学性能测试试样均为在钢管对焊后纵向取样，焊缝的化学成分见表 2。具体焊接工艺为：首先采用 ϕ2.4 mm× 1 000 mm的 Thermanit MTS911 手工氩弧焊焊丝打底，焊接预热温度为 200～250 ℃，层间温度为 250～350 ℃，采用纯氩保护，直流正接；然后采用 ϕ4 mm× 350 mm的 Thermanit MTS911 焊条电弧焊，焊条用前进行 300～350 ℃× 2 h 烘干，焊接预热温度200 ℃，层间温度为 250～350 ℃，焊接电流为200 A，采用 SS630 型松下焊机，直流反接；最后采用ϕ3 mm的 Thermanit MTS911 埋弧焊焊丝盖面，焊剂采用 Marathon543，用前进行 300～350 ℃× 2 h烘干，焊接预热温度200 ℃，层间温度 270 ℃，焊接电流 350～400 A，电压32 V，采用 NA－3S 型自动焊机直流反接，焊接速度为0.5 m/min。焊后的试样首先进行750 ℃× 3 h炉冷的消除应力热处

收稿日期：2007－10－11

理,然后进行650 ℃长时时效试验和650 ℃高温持久试验,最后机械加工成相应的试样尺寸。焊接接头的持久试验采用圆棒试样,拉伸试样为板状试样,冲击试样为夏比V形缺口试样。

表 2 E911钢焊缝的化学成分(质量分数,%)

Table 2 Chemical composition in welded joint

C	Si	Mn	P	S	Cr	Mo	
0.09	0.18	0.45	0.016	0.003	8.77	1.00	
W	Ni	V	Nb	N	Al	B	Fe
1.03	0.58	0.20	0.06	0.04	0.02	0.0006	余量

用RKP—300型示波冲击试验机进行冲击试验,用CSS—1110型电子万能试验机进行常温拉伸试验,用WG3—1050型高温长均热区试验电炉进行时效试验,CLLO 910A型六头持久试验机进行持久强度试验,试验方法按国家标准GB/T2039—97。采用英国MAGISCAN—ⅡA型图像分析仪和CAM—SCAN型扫描电镜观察断口的断裂特征,并依照国家标准GB/T12778—91有关金属夏比冲击断口的测定方法,来测定冲击断口的韧性区面积百分比。用Neopht—Ⅱ型金相显微镜进行金相组织观察及照相,组织显示用4%硝酸酒精。透射电镜试样采用MTP—1A型双喷电子减薄仪减薄,在PHILIPS CM12型透射电镜下进行观察,采用EDAX9100型能谱分析仪对碳化物进行成分测定。

2 试验结果与分析

2.1 E911钢焊接接头650 ℃长期时效前后力学性能

针对超超临界机组主蒸汽参数649 ℃的要求,文中对E911钢母材和焊接接头进行了650 ℃长达1 000,3 000,5 000 h的时效处理,然后进行力学性能测试。其650 ℃长期时效前后力学性能的变化如图1所示。从图1可看出,经过650 ℃长达5 000 h时效后,该钢的强度值 $R_{0.2}$ 和 R_b 分别由时效前的612.5和745 MPa降低到535和730 MPa;焊缝的 $R_{0.2}$ 和 R_b 分别由时效前的570和730 MPa降低到560和705 MPa;时效3 000 h时焊缝的 $R_{0.2}$ 和 R_b 最低,分别为505和645 MPa。时效3 000 h时焊缝的 $R_{0.2}$ 和 R_b 出现低谷的原因初步认为是3 000 h长时时效产生回复再结晶的结果,而时效5 000 h后晶内的碳化物析出又导致强度升高,详细的机理尚有待深入研究。

2.2 E911钢焊接接头650 ℃高温持久性能

E911钢持久强度试样采用圆棒试样,试验温度为650 ℃,最长试验时间17 647 h,母材外推10^5 h的

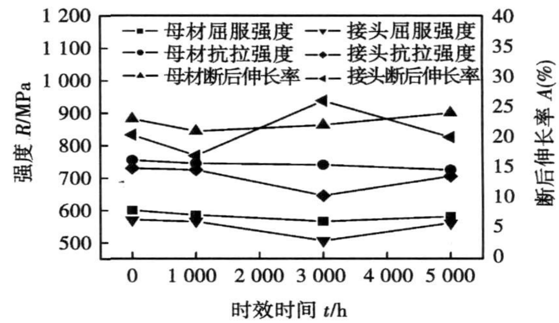

图 1 E911钢焊接接头650 ℃时效前后的力学性能

Fig. 1 Mechanics property of E911 steel welded joint around 650 ℃ long-time aged

持久强度值 R_{10^5} = 72.52 MPa(图2);E911钢焊接接头的持久强度试样最长试验时间5 511 h,外推10^5 h的持久强度值 R_{10^5} = 60.88 MPa(图3)。可看出E911钢焊接接头的持久强度值较高,该值比T91钢母材在625 ℃的外推10^5 h的持久强度值高20%。

E911钢与T91钢成分上的差别是加入了钨、硼,E911的钨含量为0.90%~1.10%,钨起固溶强化作用,并且钨降低$M_{23}C_6$碳化物长大的速度,硼起强化晶界的作用,从而提高持久强度[3]。

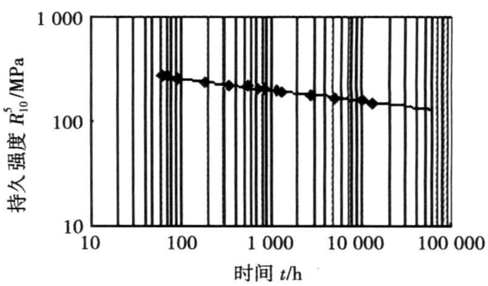

图 2 E911钢高温持久性能曲线

Fig. 2 Sustained strength curve of E911 steel at high temperature

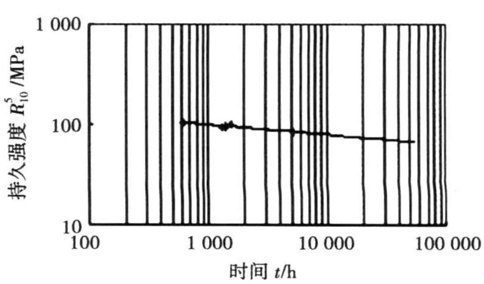

图 3 E911钢焊接接头高温持久性能曲线

Fig. 3 Sustained strength curve of E911 steel at high temperature

2.3 E911钢焊接接头650 ℃长期时效后的断口分析

对E911钢母材经650 ℃时效后的室温冲击断

口进行了观察。E911 钢母材其供货状态的断口为韧窝断口, 经650 ℃× 1 000 h时效后的冲击断口为准解理断口, 另外在断口上还观察到了二次裂纹; 经650 ℃×2 000 h时效后的冲击断口仍为准解理断口, 但其准解理面比650 ℃× 1 000 h时效的解理面大; 经650 ℃× 3 000 h时效后的冲击断口仍为准解理断口, 但撕裂岭变得很窄; 随着时效时间的延长断口的形态变化并不大, 经650 ℃× 5 000 h时效后的冲击断口仍以准解理断口为主。

E911 钢焊接接头经 650 ℃长期时效后的冲击断口的变化规律与母材的变化规律基本相同, 只是比母材的韧窝特征要少, 解理面更多、更清晰, 是典型的断口形貌。

E911 钢母材和焊接接头冲击断口的变化形貌与时效时间对冲击功的影响数据基本是吻合的, 即 E911 钢母材和焊接接头在 650 ℃× 1 000 h 时效阶段的冲击功大幅降低, 但在随后的时效过程中冲击功变化很小。

2.4　E911 钢焊接接头 650 ℃长期时效后的显微组织

图4 和图 5 分别是 E911 钢母材和焊缝时效前的试样光学金相组织形貌, 经650 ℃× 5 000 h 时效后 E911 钢焊缝和热影响区组织均较时效前组织发生细化, 由此可以推断在时效的过程中发生了回复和再结晶, 导致显微组织的细化。

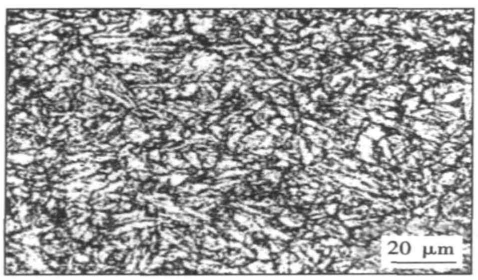

图 4　E911 钢母材的金相组织

Fig. 4　Metallograph of E911 steel

图6 和图 7 分别是 E911 钢母材和焊缝 650 ℃× 5 000 h 长期时效后观察到的位错、再结晶形成的亚晶及碳化物的透射电镜拍摄的形貌, 图 8 是对焊缝中的碳化物的能谱分析结果。可以看出, E911 钢母材中碳化物很多, 可看到碳化物有长条形、球形、小球形、小针形 4 种, 对长条形碳化物进行了能谱分析, 分析结果属 $M_{23}C_6$ 型碳化物, 条状碳化物分布在 α-Fe 边界上; 细小 MC 碳化物分布在 α-Fe 板条内部, 这两种碳化物通过沉淀强化而改善了材料持久强度。对球形碳化物的能谱分析结果, 仍属于 $M_{23}C_6$ 型碳化物, 但铬含量比长条形降低, 铁含量比长条形增加; 经能谱分析表明, 小球形碳化物的钒高, 属 MC 形碳化物, 从形状上看属于富铌的碳氮化物 M(C, N), 极细小针状碳化物的钒也高, 属 MC 形碳化物, 从形状上看属于复杂的富钒氮化物[4]。

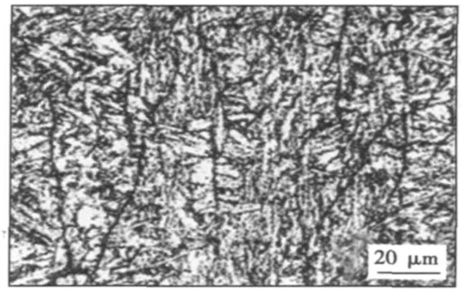

图 5　E911 钢焊缝的金相组织

Fig. 5　Metallograph of E911 steel welded joint

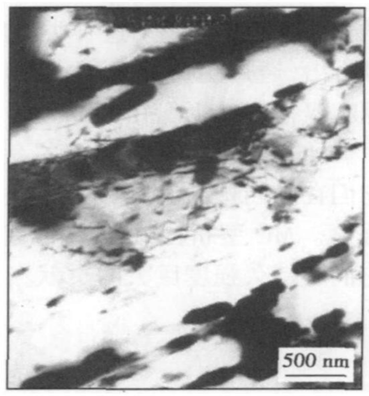

图 6　E911 钢母材中的位错和碳化物

Fig. 6　Distribution of dislocation and carbides in E911 teel

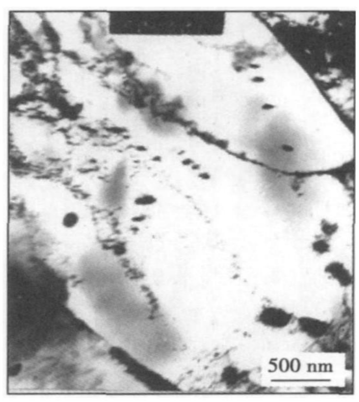

图 7　E911 钢焊缝中晶内碳化物析出

Fig. 7　Precipitated carbides in E911 steel welded joint

与母材相比可以看出: E911 钢焊缝中的 α-Fe 边界上粗大碳化物减少、位错增多及晶内细小的碳化

物增多,对E911钢焊缝中碳化物的能谱分析结果与母材的分析结相同,即晶界粗大的属 $M_{23}C_6$ 型碳化物,晶内细小的碳化物属MC型碳化物。

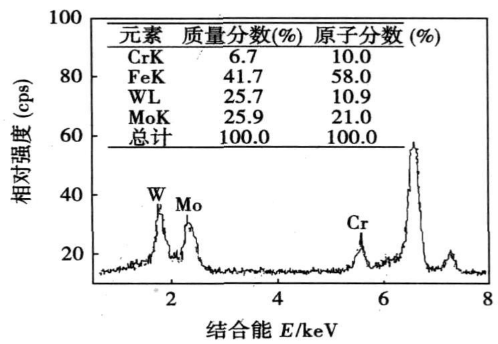

图8 E911钢焊缝中碳化物的能谱分析

Fig. 8 Analysis result of carbide by EDS in welded joint

在E911钢中的主要析出物是由Cr,Fe,Mo(W)和C组成的 $M_{23}C_6$ 型碳化物。这种类型的碳化物回火时在晶界析出,通过阻碍晶粒长大来增加持久强度,经钒、铌和氮很好的平衡在E911钢中产生了MC型析出物[5]。MC型析出物主要由钒、铌和氮组成,并且发现它们在晶内析出。在那里它们钉轧位错来提高持久强度。MC型析出物的热稳定性非常高,这能解释它们对持久强度巨大的贡献。

3 结 论

(1)E911钢焊接接头经650 ℃长期时效后仍具有很好的力学性能,表明该钢具有很好的焊接性能。

(2)E911钢有很高的持久强度,母材在650 ℃温度下持久试验数据外推 10^5 h的持久强度 R_{10^5} = 72.52 MPa;E911钢焊接接头的持久强度外推 10^5 h的持久强度 R_{10^5} = 60.88 MPa。

(3)断口分析结果表明,E911钢母材和焊接接头经650 ℃×3 000 h时效后的冲击断口为准解理断口。

(4)透射电镜观察结果表明,E911母材和焊接接头均是在马氏体基体上分布着 $M_{23}C_6$ 型碳化物MC型碳化物。经650 ℃时效后 $M_{23}C_6$ 型碳化物减少、位错增多,随着时效时间的延长发生回复与再结晶现象,从而产生亚晶粒和胞状结构,并有大量MC型碳化物的析出。

参考文献:

[1] 大神正浩,荒木敏,直井久,等. ポイラ管用9Cr-0.5Mo-1.8W钢の开发と实用化[J]. 铁と钢, 1990, 76(7): 1124-1128.

[2] 赵钦新,顾海澄,陆燕荪. 国外电站锅炉耐热钢的一些进展[J]. 动力工程, 1998, 18(1): 74-75.

[3] John Hald. Metallurgy and creep properties of new 9%~12% Cr steels[J]. Materials Technology, 1996, 67(9): 370-373.

[4] 周静彬,周立新,宛 农. T91钢合金元素对持久强度的影响[C]//第18届全国锅炉用钢会论文集,哈尔滨: 2000, 6-19.

[5] 龚正春. 超超临界锅炉用E911钢管的高温性能[J]. 理化检验-物理分册, 2003, 39(11): 552-554.

作者简介:任文超 男,1965年出生,工学硕士,高级工程师。主要研究方向为舰船材料、纳米材料。发表论文20余篇。

Email: renwenchao@hrbeu.edu.cn

Ningbo Institute of Technology, Zhejiang University, Ningbo, Zhejiang 315100, China; 2. School of Material Science & Engineering, Harbin University of Science and Technology, Harbin 150080, China; 3. State Key Laboratory of Advanced Welding Production Technology, Harbin Institute of Technology, Harbin 150001, China). p93—96

Abstract: There often be the curve welding seam (CWS) in remote welding. The accurately identified CWS is one of the prerequisites to ensure tele-teaching precision. Aiming at the characters of CWS, the concept of inflection point and direction coefficient of welding seam are put forward. The intelligent model of direction coefficient of welding seam is established. Combining with the identifying algorithm of inflection point in welding seam, identifying experiment of CWS is done. The experiment results show that inflection point of welding seam can be automatically identified, that the average error of CWS is less than ±0.5 mm by optimal treatment of off-line programming system, and meets the requirements of tele-teaching.

Key words: remote welding; tele-teaching; force sensing; curve welding seam (CWS)

Identification of multiclass defects in aluminum alloy resistance spot welding based on support vector machine XUE Haitao[1], LI Yongyan[1], CUI Chunxiang[1], AN Jinlong[2] (1. School of Materials Science and Engineering, Hebei University of Technology, Tianjin 300132, China; 2. School of Electrical Engineering and Automation, Hebei University of Technology, Tianjin 300132, China). p97—100

Abstract: A model is built to identify splash defect and incomplete fusion defect of aluminum alloy resistance spot welding based on Support Vector Machine method. The characteristic vector used in the model is extracted from process curves of aluminum alloy resistance spot welding. This model is trained and tested with different sample data. The test result shows that the accuracy rate of identifying splash defect is 96.7% and the accuracy rate of identifying incomplete fusion defect is 100% under given sample data. Therefore, it is reliable to identify multiclass defects of aluminum alloy resistance spot welding with Support Vector Machine method.

Key words: aluminum alloy resistance spot welding; support vector machine; defect identification

Influence of loading of tensile stress on welding residual stress field in plate structure PAN Hua[1], FANG Hongyuan[2] (1. Automobile Steel Department, Research Institute, Baoshan Iron &Steel Corporation Limitid Shanghai 201900, China; 2. State Key Laboratory of Advanced Welding Production Technology, Harbin Institute of Technology, Harbin 150001, China). p101—104

Abstract: By finite element method (FEM), the distribution of welding residual stress field in the plate structure was investigated under the condition of local loading, and compared the results of reducing stress between tension in process of welding and after welding. It is found that under the condition of local loading, tension in welding process can decrease the residual stress more significantly than that after welding. When the local loading was lower than the yield strength of the material, the decrease of residual stress become more prominence as the local loading increasing. When 200 MPa loading was applied, the maximum tension residual stresses decreases to 130 MPa after welding and to 50 MPa during welding. These results indicate that the decrease of welding residual stress by local loading is feasible.

Key words: welding; residual stress; finte element method; mechanical tension

Microstructure and properties of E911 steel welded joint aged at 650 ℃ for long-time REN Wenchao[1], GONG Zhengchun[2], CHANG Tiejun[3], WANG Chunbin[3] (1. School of Mechanical and Electrical Engineering, Harbin Engineering University, Harbin 150001, China; 2. Harbin Boiler Company Ltd, Qinhuangdao Hebei 066206, China; 3. College of Materials Science and Chemical Engineering, Harbin Engineering University, Harbin 150001, China). p105—108

Abstract: The mechanical properties, serial impact and sustained strength of the welded joint aged at 650 ℃ for long-time of E911 steel produced by German Vallourec &Mannesmann were tested, optical microscope, transmission electron microscope (TEM) and scanning electron microscope (SEM) were used to observe and analyze the microstructures and the fracture apptarance. The tests show that the welded joint aged at 650 ℃ for long time of E911 steel has good mechanical properties and sustained strength, the rupture strength of E911 steel is 72.52 MPa when the aging time is extended to 100, 000 hours at 650 ℃, and the rupture strength of welded joint is 60.88 MPa.

Key words: E911 steel; long-time aging; sustained strength; microstructure; mechanical properties

3D finite element simulation on distortion distribution in multi layers welding of EH36 CHEN Zhanglan, XIONG Yunfeng, LI Zongmin (Marine Engineering School Jimei University, Xiamen, Fujian 361021, China). p109—112

Abstract: As one of low temperature high strength steel, EH36 is widely used in key construction of ship. Based on the thermal-physical properties of EH36, 3D finite element simulation is carried out to analyse the temperature field and distortion distribution. To simulate the actual welding process, some technologies, such as APDL program used for development and birth & death skill, are applied in 3D multi passes welding. Thus the temperature field and weld distortion distribution in 3-directions are obtained. The result of simulation shows that there are many different distortions between the first pass and the second one, and that difference lies between the firstly welded part first and the later welded part. Further, the distortions of U-shape groove and V-shape groove were compared, the angle deformation of workpieces with V-shape groove is obviously greater than that of the U-shape groove at the same area of weld crass-section, both of them share with the same areas, same welding process and simulation process.

Key words: EH36 steel; multi-layers; distortion; simulation